JOURNAL OF PROPULSION AND POWER
Vol. 11, No. 4, July–August 1995

Analysis of Elementary Models for the Steady-State Combustion of Solid Propellants

V. A. Strunin* and G. B. Manelis†
Institute of Chemical Physics in Chernogolovka, Moscow Region 142432, Russia

An analysis is conducted of various theoretical models for the combustion of condensed systems: combustion regimes involving the destruction and dispersion of solid, foaming of the melting substance, vaporization or sublimation of decomposing substances, decomposition and oxidation of propellant components in quasihomogeneous composite systems, and heterogeneous reactions in laminated systems (chemical arcs, sandwiches). The main combustion characteristics: burning rate, burning surface temperature, dependence of burning rate on pressure and initial temperature as well as on other kinetic, thermodynamic, and physical parameters, are studied analytically and numerically. Conclusions are made about the mechanism and the leading stage of the combustion, as well as the methods of varying the combustion characteristics of different condensed systems, including explosives and solid propellants.

Nomenclature

A = pre-exponential factor, s^{-1}
a = dimensionless concentration of gaseous component
b = radius of specimens in chemical arc, cm
C = specific heat coefficient, cal/(g·K)
D = diffusion coefficient, cm^2/s
d = distance between samples in chemical arc, cm
E = activation energy, cal/mole
j = stoichiometric coefficient
K = reaction rate constant, s^{-1}
L = total sandwich layer size, $2l$, cm
M = molecular weight, g/mole
m = mass burning rate, g/cm^2s
m_0 = maximum mass burning rate of sandwich system, g/cm^2s
n = pressure exponent, $\partial \ln r/\partial \ln p$
p = pressure, atm
Q = heat of reaction, cal/g
R = gas constant, cal/(g·mole·K)
R^* = gas constant, atm·cm^3/(g·mole·K)
r = linear burning rate, cm/s
r_N = $\partial T_s/\partial T_0$
s = specific surface, cm^{-1}
T = temperature, K
T_b = combustion temperature, K
T_m = maximum combustion temperature, K
W = reaction rate, g/cm^3s
x = space coordinate, cm
Y = degree of transformation, dispersion or consumption via chemical reaction, sublimation, evaporation
y = space coordinate, cm
z = y/l
α = angle between direction of combustion wave propagation and normal to surface at a given point
δ = criterion of thermal stability of combustion
η = ratio of reaction rates in gas and condensed phases
θ_s = cT_s/Q_c
κ = criterion of thermal stability of combustion
λ = thermal conductivity coefficient, cal/(g·cm·s)
ν = kinematic viscosity coefficient, cm^2/s
ξ = x/l
ρ = density, g/cm^3
σ_p = temperature sensitivity of burning rate, K^{-1}
ϕ = linear oxidizer fraction in sandwich layer
ψ = stoichiometric coefficient

Subscripts

c = condensed phase
D = diffusion
d = dispersion
e = vaporization, sublimation
f = fuel decomposition
g = gas phase
ox = oxidation
r = decomposition reaction
s = burning surface
0 = initial
1, 2, 3 = numbers of components and reactions

Introduction

MOST fundamental works on combustion focus their attention on consideration of gas-phase reactions of both simple and complex kinetics.[1,2] Combustion models for condensed systems, in particular, for composite solid propellants, are also available.[3]

However, condensed systems are extremely diversified and complicated. Therefore, the comprehensive description of all chemical and physical processes of the combustion of condensed systems, and the solution and analysis of the mathematical problem with many parameters involve considerable difficulties which, in turn, plague the investigation of the combustion mechanism.

Historically, the first theoretical study of the combustion of energetic materials, performed by Ya. B. Zeldovich in 1942, was based on assumptions about pure gas-phase or pure condensed-phase exothermic transformations in the combustion wave. This study was in line with the understanding of the combustion mechanism of the day and with methods available for solving mathematical problems. Later, in the 1960s and 1970s, it was established experimentally that most energetic materials were able to release heat in both the gas and condensed phases, but, depending on the combustion con-

Received Nov. 28, 1994; revision received Feb. 7, 1995; accepted for publication Feb. 9, 1995.
*Dr. Sci., Leading Scientist.
†Dr. Sci., Head of Laboratory.

ditions, the leading stage could be localized in the vicinity of the burning surface or in the gas phase. This permits one to apply approximate combustion mechanisms to particular cases to describe the combustion of real condensed substances. In the present work, we present an analysis of combustion mechanisms in the condensed and gas phases. Then we consider the mechanisms of combustion of quasihomogeneous, heterogeneous, and laminated systems. Finally, some consideration is given to the combustion of composite solid propellants.

This article suggests elementary (including only the burning-rate controlling factors) combustion models, which can be used in the qualitative analysis of combustion characteristics, in determining the leading stage of combustion and in estimating the effects of particular chemical and physical processes on the burning law.

Combustion in the Condensed Phase

A chemical reaction propagating as a combustion wave in a condensed substance can be described by relations similar to those for gas-phase combustion. Note that the Zeldovich–Frank–Kamenetskii equations for the burning rate are the same for the condensed and gas phases for zero-order reactions, for which solution of the diffusion equation is not required.[4] However, as a rule, combustion of condensed substances and their compositions involves total or partial transformation of the condensed substance to gas, which is accompanied by the formation of a burning surface. Thus, account must be taken of the surface temperature. If the original substance is nonmelting, nonvolatile, and capable of exothermic decomposition in the solid state, gaseous combustion products can crush the surface layer and generate small particles forming a so-called "smoke-gas" zone. This phenomenon is termed dispersion. It was observed for the first time in the flameless combustion of primary explosives and powders at low pressures.[5]

The condensed-phase combustion is described by conventional heat and mass transfer equations excluding the mass diffusion term and neglecting the heat exchange with the gas phase (zero temperature gradient at the burning surface). The burning rate depends on the reaction rate at the burning surface temperature, which is a function of the effective heat of reaction and of the extent conversion[6]:

$$r^2 = \frac{\lambda_c R T_s^2 A_r}{\rho_c Q_c E_r I_0} \exp\left(-\frac{E_r}{RT_s}\right) \tag{1}$$

where

$$T_s = T_0 + \frac{Q_c}{C_c} Y_s, \qquad I_0 = \int_0^{Y_s} \frac{Y_s - Y}{F(Y)}\, dY$$

$I_0 = 1/2Y_s^2$ for the zero-order reaction, $F(Y) = 1$, and $I_0 = Y_s - (1 - Y_s)\cdot \ln(1 - Y_s)^{-1}$ for the first-order reaction, $F(Y) = 1 - Y$.

The amount of the dispersed substance is related to the amount of the decomposed substance at the burning surface as follows: $Y_d = 1 - Y_s$. Experiments have shown that the amount of smoke, proportional to the extent of dispersion, reduces with increasing pressure. Hence, there is a functional relation between the dispersion and the pressure dependence of the burning rate. In the simplest case, this relation can be presented[7] as follows. The destructive force of the gas motion within the subsurface layer is proportional to the pressure gradient, and correspondingly, to the filtration rate in pores. Considering the mass continuity equation and equating the destructive force and the strength of the solid at the moment of burning surface formation, we obtain a linear dependence of burning rate on pressure with a proportionality factor incorporating the combined dependencies of permeability, strength, and other parameters on solid porosity. The conclusion about the linear burning law has been supported experimentally.[5] As an illustration, Table 1 lists calculated and experimental data for the combustion of mercury fulminate.[6]

Table 1 Combustion characteristics of mercury fulminate at subatmospheric pressures

Calculation		Experiment		
Y_d	r, cm/s	T_s, K	Y_d	r, cm/s
0.76–0.66	0.1–0.58	630–770	≈0.7	0.4

Now consider combustion involving the melting of a nonvolatile substance. The released gases foam the solid and thereby extend its volume. The solid density and, hence, the heat release per unit volume decrease. The foam structure of the combustion zone was first discovered in the combustion of double-base (nitroglycerin) propellants. The theory of the process in the case of permanent transition from the density of the solid to density of the gas in the combustion wave was developed by Maximov and Merzhanov.[8] The burning rate is determined by the equation

$$(\rho_c r)^2 = \frac{2\lambda_c A_r M_g T_m p}{Q_c E_r} \exp\left(-\frac{E_r}{RT_m}\right) \tag{2}$$

which suggests that the pressure exponent $n = \partial \ln r/\partial \ln p$ must approach 0.5.

As an example, we refer to the combustion of borane hydrazine. The thermal decomposition and combustion of this compound have been studied by Manelis et al.[9] In this case, the foam stability and the decomposition at temperatures close to maximum are provided by boron nitride formed by the reaction $BH_3N_2H_4 \rightarrow BN + 0.5N_2 + 3.5H_2$ (yield ~100%). Here, we have effective intramolecular oxidation of boron, which is not complicated by diffusion. The experimental pressure dependence of the burning rate for borane hydrazine at pressures of 20–100 atm obeys the equation r (cm/s) $= 0.62p^{0.58}$ (atm). The experimental values are in good agreement with those calculated using the kinetic constants of liquid-phase decomposition.

The types of condensed-system combustion most commonly encountered are combustion of substances capable of both decomposition and evaporation (or sublimation). Among these substances are nitro compounds, nitroesters, nitramines, onium perchlorates, and nitrates, which are important components of explosives and solid propellants. Burning surface temperature, which depends on the pressure of the saturated vapor of a substance, is a criterion for the possibility of preferable decomposition of a substance in the condensed or gas phase within the combustion wave.

Let us consider a combustion mechanism involving decomposition in the condensed phase, with the gas-phase reaction rate being negligible. The burning surface formation corresponds to the instant at which the sum of the decomposition and evaporation fractions is equal to unity, the sum of partial pressures of decomposed and evaporated products is equal to unity, and the sum of partial pressures of decomposed and evaporated products is equal to external pressure. This assumption is valid provided the reactions in the gas phase are absent, or proceed at a distance far from the burning surface. It should be noted that in terms of this model, one need not resort to arbitrary assumptions concerning the burning surface parameters as was the case in some other works. Thus, we have[7,10]

$$Y_s + Y_e = 1, \qquad T_s = T_0 + (Q_c/C_c)Y_s - (Q_e/C_c)Y_e \tag{3}$$

$$p = p_r + p_e = \left(1 + \frac{M_e}{M_r}\frac{1 - Y_e}{Y_e}\right) A_e \exp\left(-\frac{E_e}{RT_s}\right) \tag{4}$$

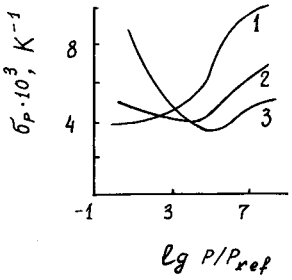

Fig. 1 Temperature sensitivity of burning rate as a function of pressure at different values of condensed-phase heat release increasing from curve 1 to curve 3.

for the zero-order reaction

$$r^2 = \frac{2\lambda_c RT_s^2 A_r \exp(-E_r/RT_s)}{\rho_c E_r(1 - Y_c)[Q_c - (Q_c + Q_e)Y_e]} \tag{5}$$

$$n = \frac{\partial \ln r}{\partial \ln T_s}\frac{\partial \ln T_s}{\partial \ln p} = \frac{(E_r/2RT_s^2)(T_m - T_s)}{1 + (E_e/RT_s^2)(T_m - T_s)} \tag{6}$$

$$\sigma_p = \frac{\partial \ln r}{\partial T_s}\frac{\partial T_s}{\partial T_0} = \frac{(E_r/2RT_s^2) + (E_e/RT_s^2)[(T_m - T_s)/(T_s - T_0)]}{1 + (E_e/RT_s^2)(T_m - T_s)} \tag{7}$$

where $T_m = T_0 + Q_c/C_c$. Under extreme conditions, i.e., at $p \to 0$, $Y_c \to 1$ and $n \to E_r/(2E_c)$, while at $p \to \infty$, $Y_c \to 0$, and $n \to 0$.

Analysis of these expressions shows that evaporation plays an important role as a limiting and stabilizing factor, and acts via the feedback mechanism. For example, the fraction of evaporation increases with increasing heat supply to the condensed phase (with increasing Q_c and T_0), and the expenditure of heat for evaporation increases, slightly enlarging the values of T_s, r, and n. In terms of this mechanism, the pressure dependence of burning-rate temperature sensitivity exhibits an unusual and rather unexpected behavior.[11] Figure 1 shows that σ_p decreases at low pressures and increases at high pressures. As a result, the pressure dependence has a minimum. Changes in the extent of heat release in the condensed phase affect σ_p at low and high pressures in different ways.

To a large extent, the σ_p value determines the thermal stability of combustion. Combustion is assumed to be stable[12] if

$$\kappa = \sigma_p(T_s - T_0) \leq 1 \tag{8}$$

or

$$\delta = \frac{(\kappa - 1)^2}{r_N(\kappa + 1)} < 1, \qquad \kappa > 1 \tag{9}$$

where $r_N = \partial T_s/\partial T_0$ and $p = \text{const}$.

For our model we have[13]

$$\delta = \frac{[(E_r/2RT_s^2)(T_s - T_0) - 1]^2}{1 + (E_r/2RT_s^2)(T_s - T_0) + (2E_e/RT_s^2)(T_m - T_s)} \tag{10}$$

Equation $\delta(T_s) = 1$, which sets the stability limit, is cubic with respect to T_s and, hence, has three roots that can be real for certain parameters and can fall within the range of acceptable T_s values. The analysis shows that for different decomposition–evaporation kinetics, the $r(p)$ curve can involve one or two combustion stability limits.

Let us analyze experimental data on the combustion of some onium salts, in particular of ammonium perchlorate (AP),[10] in terms of the above mechanism. To understand the deflagration mechanism of such compounds, it is important to clarify the mechanism and peculiarities of the combustion of composite propellants.

The pressure dependence of the burning rate for AP is distinguished by the following features. The results of measurements at 20–140 atm, reported by different authors, basically coincide. At higher pressures, the measured burning rates essentially differ, the $r(p)$ curves exhibit a somewhat unusual behavior [plateau or, $r(p)$ decrease], and high sensitivity of the burning rate to admixtures, heat losses, and other factors is observed. A number of experimental data are indicative of the importance of thermal decomposition of AP during combustion. Among these data are the foam structure of the surface layer of extinguished samples, the exothermic effect of the reaction in the condensed phase (measured by thermocouples), and the effects of ionizing radiation and catalysts on thermal decomposition.[14] However, deflagration of AP under atmospheric pressure requires approximately 100 cal/g of additional energy, most of which compensates for the heat expended for AP sublimation ($Q_c \approx 500$ cal/g). The burning rate calculated using the kinetics of solid-phase decomposition of AP ($K_r = 10^9 e^{-32{,}000/RT}\ s^{-1}$) is 0.02 cm/s, which coincides approximately with the experimental value; the calculated value of T_s (750 K) is close to the experimental value (770 K). The sublimation fraction is ~30%. At pressures of 40–100 atm, the calculated burning rate is half as large as the experimental one. This difference can be accounted for by the fact that the reaction proceeds partially in the liquid phase (perhaps the melting of AP or the formation of liquid eutectic with water), where the reaction rate can be an order of magnitude higher than the rate of solid-phase decomposition.[10,14] The characteristic features of AP combustion at high pressures seem to be accounted for by the thermal instability of the combustion (flame emissivity pulsations were observed in experiments). The calculated value of the stability criterion ($\delta > 1$) supports this assumption.

The common and specific phenomena caused by the condensed-phase decomposition in the combustion of other onium salts are as follows. The burning rate of hydroxylammonium perchlorate (HAP)[15] depends on the excess concentration of the dissociation products, hydroxylamine salt and perchloric acid. According to the kinetic data, the effect of the salt is more pronounced. Calculated combustion characteristics show good agreement with experimental data (Table 2).

The combustion of HAP is unstable at 20–100 atm; at lower and higher pressures, the process is stationary. The $\sigma_p(p)$ dependence is minimum at intermediate pressures. This behavior is consistent with the condensed-phase combustion model.

It should be noted that the unstable combustion at intermediate pressures (pulsations, decrease of pressure exponent down to negative values, extinction) is typical for the compounds under consideration and is associated with the concurrence of the decomposition and vaporization processes. This effect is most pronounced in the combustion of organic perchlorates.[13,16]

The thermal decomposition of ammonium nitrate (AN), unlike that of AP, occurs in melt. The concentration of the acid formed in AN dissociation is higher since AN is a salt of the acid weaker than perchloric; AN is a more volatile compound than AP and, hence, its burning surface temperature is lower; and, finally, the oxidation ability of AN decomposition products (nitroxides) is relatively low. As a result, AN is incapable of deflagration without catalytic additives. Table 3 lists the calculated combustion characteristics of AN and experimental data for AN doped with sodium and barium chlorides and chromium oxide.[17]

The unstable combustion of AN is detected beginning at ~400 atm. The burning rate decelerates (plateau) or even decreases with pressure, and flame pulsations are observed.

Another characteristic feature of AN combustion is the strong effect of the salts of alkaline and alkaline–Earth met-

Table 2 Combustion characteristics of HAP at 20 atm

Characteristic	r, cm/s	T_s, K	Y_c	n	$\sigma_p \times 10^3$, K^{-1}	δ
Calculation	0.21	830	0.50	0.48	3.2	1.35
Experiment	0.28	780 ± 60	——	0.50	3.5	Unstable

Table 3 Combustion characteristics of AN at 70 atm

Characteristic	r, cm/s	T_s, K	Y_c	n
Calculation	0.34	790	0.51	1.04
Experiment	0.3–0.6	——	——	0.8–0.9

Table 4 Combustion characteristics of HN at 50 atm

Characteristic	r, cm/s	T_s, K	Y_c	n	$\sigma_p \times 10^3$, K^{-1}
Calculation	0.70	882	0.68	0.90	2.5
Experiment	0.82	860	——	0.82	3.1

als, which, in fact, do not accelerate the thermal decomposition of AN. The effect of this mechanism is discussed below in analyzing the combustion of hydrazonium nitrate (HN).

The combustion of HN at 30–120 atm pressure obeys the law,[18] r (cm/s) = $0.033p^{0.82}$ (atm). Adding potassium, sodium, lithium nitrates, or calcium chloride, increases the burning rate, but only weakly affects the lower limit of the steady-state combustion. At intermediate pressures, the acceleration effect increases from potassium nitrate to sodium nitrate and is maximum with lithium nitrate. Maximum acceleration is observed at ~10% concentrations of the additives. The acceleration effect decreases with increasing pressure, with the maximum shifting toward lower concentrations.

The HN combustion characteristics calculated using the kinetic constants for the liquid-phase HN decomposition show good agreement with experimental data (Table 4).

The accelerating effect of the above additives can be accounted for when the combustion model assumes the following mechanism. Early in the combustion, a nonvolatile additive accumulates on the burning surface. Then, in the steady-state process (when the accumulation–entrainment equilibrium is established), the additive concentration becomes higher than that in the initial composition. As a result, the pressure of saturated HN vapor must decrease, with the surface temperature (according to Raoult's law) and burning rate increasing. This assumption is supported by the analysis of potassium ions in the surface layers of extinguished samples, whose concentration was approximately three times higher than that in the original samples, and by measurements of the burning surface temperature that were higher in doped HN samples. The temperature was measured by microthermocouples.

To summarize the consideration of the condensed-phase combustion, the following conclusions can be made:

1) The combustion mechanism of heavy volatile oxidizers (onium salts) involves the combined effect and competition of two processes: 1) exothermic decomposition and 2) vaporization (sublimation), which control and stabilize the combustion.

2) This mechanism is adequate to explain combustion stability and burning rate dependence on pressure, initial temperature, and additives.

3) Surface layer dispersion occurs mainly at low pressures (<1 atm) and may contribute to a certain extent to decreasing the burning rate and increasing the pressure exponent.

4) Gas-phase reactions must also contribute to the combustion characteristics. This problem is discussed in the following section.

Combustion in Condensed and Gas Phases

The gas-phase combustion theory can readily be applied to the combustion of a condensed substance if the substance is volatile and its thermal decomposition rate in the condensed phase is low (the Belyaev–Zeldovich mechanism).[1] However, most substances used in propellants are characterized by comparable decomposition abilities in the condensed and gas phases. This kind of combustion, referred to as combined, is of great interest to researchers, but at the same time presents certain difficulties in mathematical modeling. Realization of the combined combustion mechanism for a wide range of parameters (e.g., pressure) is determined by the fact that the condensed-phase reaction proceeds at a high density of the substance, but at a temperature much less than maximum, and that the reaction rate increases with pressure due to increasing T_s, while the gas-phase reaction occurs at a lower density, but at higher temperatures, with the reaction rate increasing with pressure according to the usual mechanism of gas-phase reactions. Thus, the rates of both reactions change in the same direction.

The problem of the combined combustion is conventionally solved using the concept of flame stand-off distance. Although such an approach is rather simple, it has certain disadvantages that limit its application. First, because the functional dependence of the flame stand-off distance on determining parameters is derived from dimensionality considerations and is oversimplified, a special analysis of this dependence and its numerical justification is required. Second, the applicability of this approach is confined to a combustion regime in which the flame stand-off distance and preheating zone are the same size and are inadequate to describe other combustion regimes that can occur under a variation of parameters of the problem.

A general method for solving the problem of two-stage combustion, based on the classical approximate approach of Zeldovich–Frank–Kamenetskii, has been proposed by Vilyunov.[19] The unknown parameter comprises the burning rates in the condensed and gas phases. The complexity of the solution lies in the fact that in the first case, T_s is included in the exponential dependence and can significantly affect the burning rate, while in the second case, T_s is incorporated into the linear dependence and has a weak effect on the burning rate.

Let us use the above considerations to analyze possible combustion regimes for a substance capable of decomposition in both phases and vaporization (sublimation), e.g., for AP or HMX. The combustion is described by the following system of equations (assuming $c = c_g = c_c$):

In the condensed phase ($x < 0$)

$$\lambda_c \frac{d^2T}{dx^2} - cm \frac{dT}{dx} + Q_c W_r - Q_e W_e = 0 \qquad (11)$$

$$-m \frac{dY}{dx} + W_r = 0 \qquad (12)$$

In the gas phase ($x > 0$)

$$\lambda_g \frac{d^2T}{dx^2} - cm \frac{dT}{dx} + Q_g W_g = 0; \qquad (13)$$

$$D\rho_g \frac{d^2Y}{dx^2} - m\frac{dY}{dx} + W_g = 0 \tag{14}$$

The boundary conditions are

$$\begin{aligned} x &= -\infty, \quad Y = 0, \quad T = T_0 \\ x &= +\infty, \quad Y = 1, \quad T = T_b \end{aligned} \tag{15}$$

At the gas–solid interface, the conditions of continuity of temperature, heat flux, and mass flow are met.

Assuming that the gaseous decomposition products in the pores of the condensed phase are mixed with the vapor of the initial substance, vaporization rate W_e is expressed via decomposition rate W_r and evaporation fraction Y_e:

$$W_e = [Y_e/(1 - Y_e)]W_r \tag{16}$$

At the burning surface, we have

$$p = \left(1 + \frac{M_e}{M_r}\frac{1 - Y_e}{Y_e}\right) A_e \exp\left(-\frac{E_e}{RT_s}\right) \tag{17}$$

Three possible combustion regimes are considered in the following[20]:

1) The gas-phase reaction rate is low. The combustion takes place in the regime of separation, also referred to as the self-ignition or induction regime. The leading process is the decomposition in the condensed phase. Dividing the condensed phase[1] into preheating and reaction zones, one may derive the following equation for the burning rate (zero-order reaction):

$$m^2 = \frac{2\lambda_c(RT_s^2/E_r)\rho_c A_r \exp[-(E_r/RT_s)]}{(1 - Y_c)[2c(T_s - T_0) - Q_c(1 - Y_c) + Q_eY_e} \tag{18}$$

For the preheating zone in the gas phase, the conductive term in the energy equation may be neglected. In this case, proceeding from the equality

$$cm\left.\frac{dT}{dx}\right|_{x=0^+} = Q_gW_g \tag{19}$$

we obtain the following expression for the burning rate, which is simultaneously an additional condition for determining T_s:

$$m^2 = \frac{\lambda_g(Q_c + Q_e)(M_e/RT_s)A_gA_e \exp\{-[(E_g + E_e)/RT_s]\}}{c[c(T_b - T_0) - Q_c(1 - Y_c) + Q_eY_e]} \tag{20}$$

2) In the mixed combustion regime, the reaction rates in the condensed and gas phases are of the same order, and have a collective effect on the combustion characteristics. The equation for the burning rate in the condensed phase is the same as in region 1, while for the gas-phase burning rate we have

$$m^2 = \frac{2\lambda_gQ_gRT_b^2(M_e/RT_b)\cdot A_e \exp[-(E_e/RT_s)]\cdot A_g \exp[-(E_g/RT_b)]}{E_g[c(T_b - T_0) - Q_c(1 - Y_c) + Q_eY_e]^2} \tag{21}$$

3) In the conjunction combustion regime, where the gas-phase reaction zone is close to the burning surface, the equation for the gas-phase burning rate takes into account the reaction rate in gas at the temperature of the burning surface:

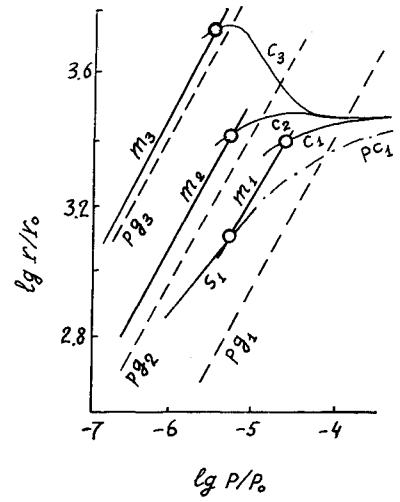

Fig. 2 Dimensionless pressure dependence of burning rate at different $\eta \sim K_g/K_c$: η = 1) 0.1, 2) 1.0, and 3) 10. Particular combustion regimes: *s*, separation; *m*, mixed; *c*, conjunction; *pg*, pure gas-phase; *pc*, pure condensed-phase.

It is convenient to perform the calculation of the parameters m, n, and σ_p as follows. T_s is considered an independent variable. Y_c is determined by equating the burning rates in both phases. Then the values of m and p are found.

Figure 2 shows the burning rate dependencies for different values on η, which is proportional to the ratio of the reaction rate constants for the condensed and gas phases. The separation combustion regime at low pressures changes to the mixed combustion regime at intermediate pressures, and at high pressures goes to the conjunction combustion regime. The transition points between the regimes are marked with circles. An increase in η results in the extension of the region of mixed combustion and shifts the separation regime towards very low pressures. In the regime of conjunction at high η, the $r(p)$ curve has a maximum because the burning rate increase due to the high rate of the gas-phase reaction changes to a decrease owing to transition to the condensed-phase combustion where the reaction rate is lower.

The numerical solution of this problem[21] has validated the approximate method. The difference in the burning rate values obtained analytically and numerically averages ~20%.

An analysis of calculation results has shown that the mass burning rate can be represented approximately as a sum of the condensed-phase or gas-phase burning rates, where each burning rate value calculated neglects the effect of the other phase entirely. This rule is accurate for no less than 15% for the ratio r_c/r_g ranging from 0.21 to 21.

Combustion of Quasihomogeneous Composite Propellants

To analyze the role of the main chemical processes proceeding in the condensed phase of combustion, consider the combustion of a model composite mixture of a fine-grained oxidizer and a polymeric fuel.[14,34] The combustion process involves the consecutive–parallel reactions of thermal decomposition of oxidizer Q_1, W_1, destruction and gasification of fuel Q_2, W_2, and its oxidation by oxidizer decomposition products Q_3, W_3. The oxidizer (like AP) transformation in the condensed phase, considered to be the leading process since the oxidizer comprises 80–90% propellant mass and is capable of independent combustion, makes the major contribution to

$$m^2 = \frac{2\lambda_gQ_gRT_b^2(M_e/R^*T_b)\cdot A_e \exp[-(E_e/RT_s)]\cdot A_g\{\exp[-(E_g/RT_b)] - \exp[-(E_g/RT_s)]\}}{E_g[c(T_b - T_0) - Q_c(1 - Y_c) + Q_eY_c]^2} \tag{22}$$

the thermokinetic mechanism of the combustion in the condensed phase.

The combustion in the condensed phase is described by the equations

$$\lambda_c \frac{d^2T}{dx^2} - cm\frac{dT}{dx} + Q_1W_1 - Q_2W_2 + Q_3W_3 = 0 \quad (23)$$

$$-m\frac{dY_1}{dx} + W_1 = 0, \qquad -m\frac{dY_2}{dx} + W_2 = 0$$
$$-m\frac{dY_3}{dx} + W_3 = 0 \quad (24)$$

The boundary conditions are

$$x = \infty, \quad Y_1 = Y_2 = Y_3 = 0, \quad T = T_0$$
$$x = 0, \quad \frac{dT}{dx} = 0 \quad (25)$$

The first integral of the energy equation gives the heat balance at the burning surface:

$$c(T_s - T_0) = Q_1Y_{1s} - Q_2Y_{2s} + Q_3Y_{3s} \quad (26)$$

For the burning rate we have

$$m^2 = \frac{2\lambda_c \int_{T_0}^{T_s} (Q_1W_1 - Q_2W_2 + Q_3W_3)\,dT}{c^2(T_s - T_0)^2} \quad (27)$$

The fraction of oxidizer decomposition Y_{1s} depends (as in the combustion model for a neat substance) on vaporization, while the fractions of fuel destruction and oxidation can be determined by dividing the kinetic equations by W_1, followed by integration:

$$Y_{2s} = \int_0^{Y_{1s}} \frac{W_2}{W_1}\,dY_1 \cong \frac{W_2(T_s)}{W_1(T_s)}\,Y_{1s}$$
$$Y_{3s} = \int_0^{Y_{1s}} \frac{W_3}{W_1}\,dY_1 \cong \frac{W_3(T_s)}{W_1(T_s)}\,Y_{1s} \quad (28)$$

Consider now the simplest chemical heat release functions

$$W_1 = \rho_c A_1 \exp[-(E_1/RT_s)]$$
$$W_2 = \rho_c A_2 \exp[-(E_2/RT_s)] \quad (29)$$
$$W_3 = \rho_g A_3 \exp[-(E_3/RT_s)]$$

The diffusion effect on the oxidation of fuel can be taken into account as follows:

$$W_3 = \rho_g S\sqrt{D_c A_3 \exp[-(E_3/RT_s)]} \quad (30)$$

for melting fuels; and

$$W_3 = \frac{\rho_g S K_D K_3}{K_3 + K_D} \quad (31)$$

where $K_D \sim D_g$, $K_3 = A_3 \exp[-(E_3/RT_s)]$ for solid fuels.

An analysis of the previous expressions allows the following conclusions:

1) An increase in the rate of oxidizer decomposition produces a double effect: it increases the burning rate ($m \sim \sqrt{W_1}$) and decreases it due to the reduced portion of oxidized fuel ($Y_{3s} \sim W_3/W_1$). It follows that if the oxidizer decomposition is so fast that the fuel has no time to react with the gaseous oxidizer in the condensed phase and the heat flux from the gas phase does not compensate the heat expenditure for preheat and gasification of the fuel, the burning rate can decrease by adding the fuel to such an oxidizer.

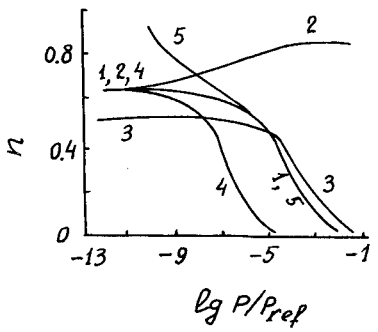

Fig. 3 Pressure exponent of burning rate as a function of pressure for quasihomogeneous propellants: 1) oxidizer; 2–5) are composite propellants: 2) $E_3 > E_1$, 3) $E_3 < E_1$, 4) $E_2 > E_1$, and 5) $E_2 < E_1$.

2) An increase in fuel gasification (decomposition, vaporization) rate decreases the burning rate since these processes take up the heat and decrease the portion of oxidized fuel.

3) An increase in the rate of fuel oxidation leads to an increase in burning rate and can be provided by increasing the reaction rate constant, extending the specific surface of the contact of components, and increasing the concentration of oxidizer gas. For this purpose, a sufficiently thermostable fuel can be used containing active groups that oxidize rapidly in the condensed phase to release a considerable amount of heat. It should be noted that the efficiency of fuel oxidation and heat release in the condensed phase is, in terms of the effect on burning rate, much higher than that in the gas phase since the heat supply to the burning surface reduces drastically with the distance from the surface to the heat release zone.

The influence of the kinetic parameters on the burning rate pressure exponent is shown in Fig. 3. For a neat oxidizer, n decreases with pressure because of reduced vaporization. The value of n increases on addition of a fuel oxidizing at an activation energy higher than that of oxidizer decomposition. Otherwise, the n value decreases. The fuel decomposition shows a behavior opposite to the above trends. The ratio of the kinetic parameters of the reactions in the condensed and gas phases also affects burning-rate temperature sensitivity and combustion stability at various pressures.

To illustrate application of the kinetic approach, consider the combustion of a propellant consisting of fine grains of AP (<50 μm) plasticized with butyl rubber, and different ferrocene catalysts.[22] The thermal decomposition of this model propellant was studied by means of differential calorimetry in sealed glass ampules. The process involves two stages: 1) the oxidizer reacts with a ferrocene compound, and 2) the catalytic oxidation of fuel components occurs. The kinetic constants obtained were used in calculating the combustion characteristics. It has been established that the first stage is completed in the initial stage of the combustion wave, perhaps, in the preheating zone. The second stage proceeds in the main reaction zone, but is limited by oxidizer sublimation. The calculation results and experimental data on burning rate and pressure exponent are summarized in Table 5.

Figure 4 shows experimental and theoretical dependencies of the burning rate on the concentration of alkyl-substituted ferrocene. It can readily be seen that the specific features of thermal decomposition kinetics and the structure of the catalyst affect the burning rate.

Combustion of Laminated Systems

Laminated systems modeling composite propellants widely used in investigations include a sandwich-like system consisting of oxidizer and fuel layers arranged normal to the combustion front,[23] and a so-called "chemical arc," a system con-

Table 5 Combustion characteristics of the composition of AP (85%), butyl rubber (15%), and dimethyl ferrocene (3% above 100%) at 40 atm

T_s, K	$c(T_s - T_0)$, cal/g	Y_s	r, cm/s		n	
Calculated	Calculated	Calculated	Calculated	Experimental	Calculated	Experimental
1000	210	0.28	1.1	1.9	0.46	0.40

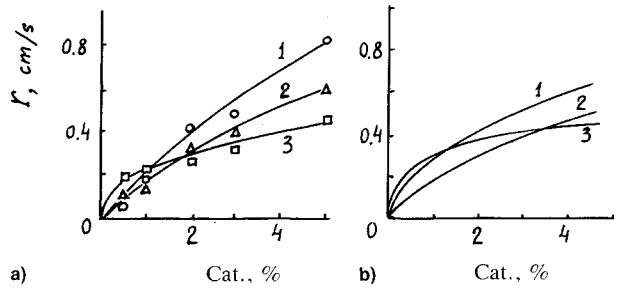

Fig. 4 Burning rate increase as a function of catalyst concentration (cat) at 40 atm: a) experiment and b) calculation. 1) Dimethyl ferrocene, 2) diethyl ferrocene, and 3) diisopropyl ferrocene.

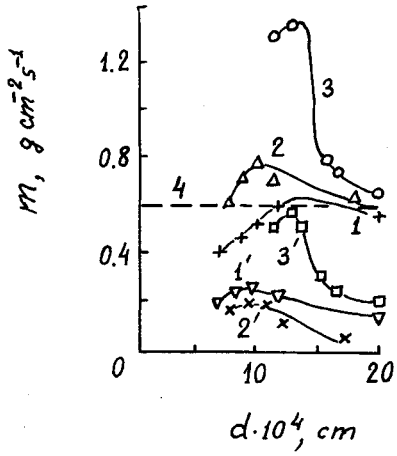

Fig. 5 Regression rates of components in a chemical arc vs distance between specimens at 40 atm. AP 1) and PMMA 1′); AP 2) and polyethylene 2′); AP 3) and graphite 3′); neat AP 4).

sisting of oxidizer and fuel bars fixed on an imaginary axis with a known gap between the end-faces.[24]

Consider first the chemical arc model for the case of heterogeneous oxidation of a solid fuel and gasification (decomposition or sublimation) of a solid oxidizer. The combustion is described by a system of the equations of heat and mass transfer written for the gas-filled gap between the end faces, with appropriate boundary conditions written for the surface of components.[25] The following relationships have been obtained for the mass regression rates of components (for the Nusselt number close to unity):

$$m_2 = \psi\rho_g A_2 \exp\left(-\frac{E_2}{RT_{2s}}\right)\frac{Q_2 + jQ_1 - (1+j)c(T_{2s} - T_0)}{Q_2 - Q_1} \tag{32}$$

$$m_1 = \frac{Q_2 - c(T_{2s} - T_0)}{c(T_{1s} - T_0) - Q_1}\cdot m_2 \tag{33}$$

The distance between the components is determined as follows:

$$d = \frac{\lambda_g(Q_2 - Q_1)(T_{2s} - T_{1s})}{\psi\rho_g A_2 \exp[-(E_2/RT_{2s})][Q_2 + jQ_1 - (1+j)c(T_{2s} - T_0)][Q_2 - c(T_{2s} - T_0)]} \tag{34}$$

The value of T_{2s} is derived from this equation. The value to T_{1s} is determined from

$$\rho_g \frac{Q_2 + jQ_1 - (1+j)c(T_{2s} - T_0)}{Q_2 - Q_1} = A_e \exp[-(E_e/RT_{1s})] \tag{35}$$

for sublimation, and

$$\frac{\psi[Q_2 + jQ_1 - (1+j)c(T_{2s} - T_0)][Q_2 - c(T_{2s} - T_0)]}{(Q_2 - Q_1)[c(T_{1s} - T_0) - Q_1]} = \frac{A_1 \exp[-(E_1/2RT_{1s})]}{\rho_g A_2 \exp[-(E_2/RT_{2s})]} \tag{36}$$

for decomposition.

The dependence of d on the force of sample pressing F is determined by

$$F = \int_0^b (p - p_0)2\pi y\, dy = \frac{3}{2}\frac{\pi\nu b^4(m_1 + m_2)}{d^3} \tag{37}$$

Figure 5 presents experimental data on the combustion of samples of AP and different fuels in a chemical arc,[26] which support the theoretical predictions, in particular, the curve maximum determined by transition from the kinetic mode of combustion to the diffusion mode.

Two variations of the sandwich model are considered: one with averaged characteristics in each layer, and the other in terms of a two-dimensional problem.[27-29] All chemical processes are assumed to take place on the surfaces of the components (heterogeneous combustion). The combustion involves the thermal decomposition and sublimation of the oxidizer and the decomposition and oxidation of the fuel.

In the first variant, the condensed-phase and gas-phase interactions of components are taken into account via heat and mass exchange coefficients. Figure 6 shows a calculated dependence of the burning rate on the size of the sandwich. At small L, the combustion is quasihomogeneous. At large ϕ values, r increases with increasing L. The "anomalous" behavior of the dependence $r(L)$ is caused by the increasing temperature at the fuel surface. With further increase in L, the behavior of the dependence $r(L)$ becomes normal. The decrease in r is associated with the reduced supply of oxidizer gas by diffusion. At a certain L, the burning rate is lower than that of the neat oxidizer burning without fuel. Finally, at sufficiently high L, the second anomalous branch appears, due to the decreased fuel effect and transition to the self-sustaining combustion of the oxidizer ($L \to \infty$).

The complex dependencies of r, n, and σ_p on p and L, predicted by the combustion model for laminated systems, have also been partially supported by the experimental results.[23,27]

The two-dimensional formulation of the problem allows one to investigate the front structure of the combustion as well as the combustion regimes, which cannot be predicted

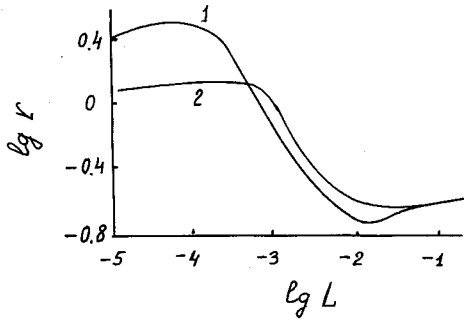

Fig. 6 Burning rate as a function of sandwich size. ϕ = 1) 7 and 2) 0.9.

within the framework of an averaged model. The virgin surface is initially considered flat. Temperatures and concentrations at the burning surface are determined first. Proceeding from particular chemical reactions at the surface (we restrict ourselves to considering the reactions of oxidizer decomposition and fuel oxidation), we calculate the local reaction rates for each point of the surface and its shape. For the convenience of calculations, we use a coordinate system with $x = 0$ corresponding to the middle of the oxidizer layer, and $x = l$ corresponding to the middle of the fuel layer. The overall size of the sandwich is $L = 2l$.

The equations for the gas-phase are as follows ($y > 0$):

$$\lambda_g \left(\frac{\partial^2 T}{\partial x^2} + \frac{\partial^2 T}{\partial y^2}\right) - cm_0 \frac{\partial T}{\partial y} = 0 \tag{38}$$

$$\rho_g D \left(\frac{\partial^2 a}{\partial x^2} + \frac{\partial^2 a}{\partial y^2}\right) - m_0 \frac{\partial a}{\partial y} = 0 \tag{39}$$

The energy equation for the condensed phase ($y < 0$) is

$$\lambda_c \left(\frac{\partial^2 T}{\partial x^2} + \frac{\partial^2 T}{\partial y^2}\right) - cm_0 \frac{\partial T}{\partial y} = 0 \tag{40}$$

The boundary conditions are the following:

at the oxidizer surface ($y = 0$, $0 \le x \le \phi l$)

$$\lambda_c \left.\frac{\partial T}{\partial y}\right|_{0^-} = \lambda_g \left.\frac{\partial T}{\partial y}\right|_{0^+} + Q_c m_r, \quad a_s m_0 - \rho_g D \left.\frac{\partial a}{\partial y}\right|_0 = \psi m_0 \tag{41}$$

$$m_r = A_r \exp[-(E_r/RT_s)] \tag{42}$$

and at the fuel surface ($y = 0$, $\phi l \le x \le l$)

$$\lambda_c \left.\frac{\partial T}{\partial y}\right|_{0^-} = \lambda_g \left.\frac{\partial T}{\partial y}\right|_{0^+} + Q_{ox} m_{ox}, \quad a_s m_0 - \rho_g D \left.\frac{\partial a}{\partial y}\right|_0 = j m_0 \tag{43}$$

$$m_{ox} = a_s \rho_g A_{ox} \exp[-(E_{ox}/RT_s)] \tag{44}$$

The symmetry conditions are

$$x = 0 \text{ and } x = l, \quad \frac{\partial T}{\partial x} = \frac{\partial a}{\partial x} = 0 \tag{45}$$

The conditions in front of and behind the combustion wave are

$$y = \infty, \quad \frac{\partial T}{\partial y} = 0, \qquad Y = +\infty, \quad \frac{\partial T}{\partial y} = \frac{\partial a}{\partial y} = 0 \tag{46}$$

The solution has the form

$$a_s = a_\infty + \frac{4(\psi + j)}{\pi} \sum_{k=1}^{\infty} \frac{\sin(k\pi\phi)\cos(k\pi x/l)}{k[1 + \sqrt{1 + (2\pi k\lambda_g/clm_0)^2}]} \tag{47}$$

$$T_s = T_\infty - \frac{2(Q_{ox} - Q_c)}{c\pi} \times \sum_{k=1}^{\infty} \frac{\sin(k\pi\phi)\cos(k\pi x/l)}{k[\sqrt{1 + (2\pi k\lambda_g/clm_0)^2} + \sqrt{1 + (2\pi k\lambda_c/clm_0)^2}]} \tag{48}$$

where $a_s = a_\infty = \psi\phi - j(1 - \phi)$ and $T_\infty = T_0 + \phi Q_c/c + (1 - \phi)Q_{ox}/c$.

The profile of the burning surface is determined from the relationship $m = m_0 \cos\alpha$, where α is the angle between the direction of combustion wave propagation and normal to the surface at a given point. Since $dy/dx = tg\alpha$

$$y = \int_{x_0}^{x} \frac{\sqrt{1 - (m/m_0)^2}}{m/m_0}\, dx \tag{49}$$

where the coordinate corresponding to the maximum m_0 is taken as x_0.

Figure 7 shows the profiles of concentration a_s, temperature $\theta_s = cT_s/Q_c$, oxidizer decomposition rate r_r, fuel oxidation rate r_{ox}, and burning surface $z = y/l$ for two L values. The maximum burning rate for the lower L value depends on the fuel oxidation rate and is located at the fuel-oxidizer interface. At the larger L, oxidizer decomposition becomes the preeminent process, however, the maximum rate remains at the interface. At certain values of the kinetic parameters, the maximum fuel oxidation rate r^*_{ox} can appear at a finite distance from the interface (Fig. 7) and its position is determined by

$$\frac{1}{r_{ox}} \frac{\partial r_{ox}}{\partial x} = \frac{1}{a_s} \frac{\partial a_s}{\partial x} + \frac{E_{ox}}{RT_s^2} \frac{\partial T_s}{\partial x} = 0 \tag{50}$$

At large L, the oxidation rate can decay to zero even within a fuel layer. Therefore, the values of a_∞ and T_∞ are calculated as corrected for incomplete combustion. This reduces to a certain extent the incorrectness of the model, which is rather qualitative in character.

A comparison of the two-dimensional calculations with the results obtained in terms of the averaging model has shown good qualitative agreement for the dependence $r(L)$. The main difference is that in the averaging model, r_{ox} decays to zero at a certain finite L value and r_r (passing its minimum) asymptotically tends to the burning rate of oxidizer without

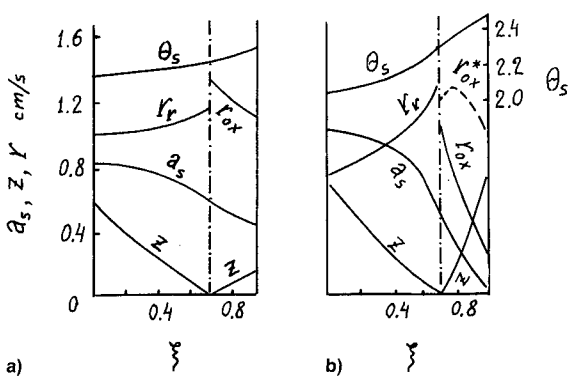

Fig. 7 Distribution of combustion characteristics over burning surface of a sandwich system (oxidizer is left of dashed-dot line, fuel to right). L = a) 5.1 × 10^{-4} and b) 2.6 × 10^{-3} cm.

fuel, while in the two-dimensional model the rate takes its minimum value characteristic of r at the interface as $L \to \infty$.

In the case in which fuel oxidation proceeds with little thermal effect, the leading process is oxidizer decomposition, and the maximum rate together with the leading point appear in the center of the oxidizer layer.

The burning surface shapes and combustion regimes predicted by the model correspond to the data of experimental studies.[30] Several authors have also stated that for AP-based propellants, oxidizer particles at low pressures protrude from the burning surface, and at high pressures form cavities.

Combustion of Composite Propellants

It is known that oxidizer deflagration essentially affects the combustion mechanism in composite propellants based on AP or similar salts. Hence, preparatory to developing a detailed mathematical theory of composite–propellant combustion that would take into account chemical, thermal, and mass interactions of components, we shall first analyze the peculiarities of oxidizer combustion and their role in the combustion of propellants.

From the above, it appears that the exothermic decomposition of oxidizer in the condensed phase is the leading process of the combustion. The calculated and experimental burning rates of onium oxidizers as a rule show good agreement and are arranged in the same sequence in magnitude. The burning rates for most composite propellants are of the same order of magnitude as the burning rate of oxidizer. Let us consider the pressure dependence of the burning. Drawing a smoothing spline through experimental points followed by calculating the value of the pressure exponent n in any narrow pressure range yields additional valuable information about the combustion mechanism.[31,32] An analysis of the numerous experimental data obtained by the authors and reported in the literature has shown that the dependence $n(p)$ for pure AP and many AP-based composite propellants is maximum within the pressure range 20–40 atm (Fig. 8). The combustion models investigated that involve parallel[33] and consecutive reactions suggest that an $n(p)$ curve can have a maximum if the pressure dependencies of the burning rates of different processes and their thermal effects are different. The change of the maximum combustion temperature with pressure (when $\partial T_b/\partial p \neq 0$) also contributes to the total value of the pressure exponent.

The minimum pressure dependence of burning rate temperature sensitivity is determined by the competition between condensed-phase decomposition and sublimation of the oxidizer. Such an unusual dependence can be obtained only within the framework of the combustion model for the condensed phase. Unfortunately, σ_p is usually measured in a relatively narrow range of combustion conditions (pressure, initial temperature). Nevertheless, in some experiments, the $\sigma_p(p)$ curves showed minima or sections with σ_p increasing or decreasing with pressure in the combustion of oxidizers (AP, HAP) and AP-based propellants with polymeric fuels and propellants doped with nitramines, metals, and catalysts.[35]

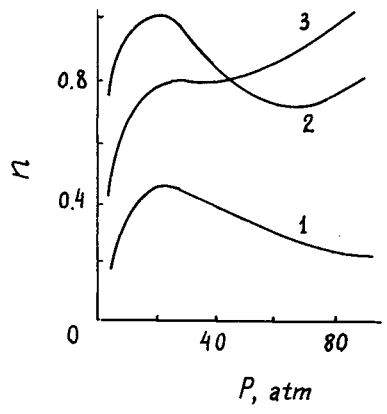

Fig. 8 Pressure dependence of the pressure exponent of burning rate for composite propellants. 1) AP + polymethylmethacrylate, 2) AP + polystyrene, and 3) AP + bitumen (according to the data of Bakhman and Belyaev[23]).

The combustion mechanism in which oxidizer transformation is a determining process is best realized in highly homogeneous compositions or in compositions involving coarse oxidizers and inert fuels.

In many cases, however, the chemical, thermal, and diffusion interactions of the oxidizer and its decomposition products with fuel components give rise to qualitatively new phenomena. From this viewpoint, let us consider burning rate as a function of the characteristic size of the components of a composite propellant.

According to the conventional concept of a combustion mechanism of composite propellants, the burning rate must monotonously decrease with increasing size since, according to the gas-phase combustion theory, the time of diffusion mixing of reagents is extended. In addition, according to the condensed-phase theory, the reaction rate decreases due to the reduced specific surface of the particles. The complex behavior of the $r(L)$ curve with two extremes, revealed in the sandwich system (Fig. 6), suggests that the combustion of composite propellants also involves a change in both combustion regimes and leading processes when the oxidizer grain size is varied. The kinetic combustion regime, with transformation of the leading oxidizer in a quasihomogeneous composition, changes to diffusion-kinetic combustion with an increasing fuel oxidation that leads to heat-exchange combustion in which the fuel is inert. Finally, there is autonomous combustion of the oxidizer or, under appropriate conditions, combustion at the oxidizer–fuel interface. As a result, pressure dependence of the burning rate changes with variations in particle size according to changing combustion regimes. This is consistent with the various shapes of the experimental $r(p)$ curves[23] (including those with plateaus where the burning rate decreases or increases as is characteristic of nitramine-containing propellants[34]), and is the result of the transition from the heat-exchange regime to the autonomous combustion of nitramine.

Referring to Fig. 8, we see that at high pressures the pressure exponent for some propellants increases (the "tail" effect). The extent of the pressure exponent increase, as shown by experimental data, depends on the intensity of the interaction between oxidizer and fuel or between their decomposition products, which in turn is determined by the particle size of components, the thermal stability and calorific value of fuel, the reactivity of catalytic additives, etc. Figure 8 shows that as the thermal stability of fuel and the probability of its oxidation in the condensed phase increase, the dependence $n(p)$ with a maximum (polymethyl methacrylate-containing composition) transforms into the curve with two extremes and a tail (the polystyrene-containing composition) and into the curve with an inflection (the bitumen-containing composition).

Interesting results have been obtained through investigation of the dependence of combustion characteristics on the properties of fuels, catalysts, and other propellant components. In particular, a natural change was observed in the characteristics of a composite propellant with alkyl-substituted ferrocene. Another example is the burning-rate variation, which depends on the way in which the catalyst (potassium permanganate) is incorporated into the composition. The burning rate decreases if the catalyst is introduced isomorphously into AP crystals and increases if the AP particles are coated with potassium permanganate; this can be accounted for by the increased dispersion of AP during burning in the first case, and by the catalytic effect of potassium permanganate in the second case.

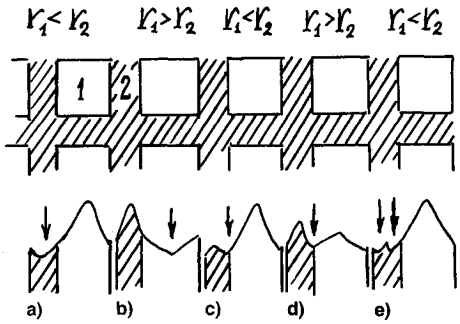

Fig. 9 Burning surface structure for different combustion regimes of a composite propellant.

Taking into account the above reasoning, let us present possible combustion regimes and corresponding burning surface structures for an ordered composite propellant (Fig. 9). In Figs. 9a and 9b, only thermal interaction occurs between components and the combustion wave propagates through a fast burning matrix with a leading point in the middle of the layer or through fast burning oxidizer particles where the leading point is in the center of each particle, followed by the consumption of fuel lamina according to the relay race mechanism.[23] In Figs. 9c–9e, a particle–matrix interaction takes place (e.g., oxidation, catalysis) and the combustion wave propagates along the interface or at a finite distance from it. The hollow on the burning surface can be asymmetric because of different regression rates of components. The burning surface can also have two hollows (Fig. 8e).

Conclusions

Current knowledge concerning the combustion of energetic materials permits us to formulate several principles that should be taken into account in combustion modeling.

1) The processes that take place within the condensed phase (thermal decomposition, oxidation, catalysis, evaporation, etc.) should be considered along with the gas-phase processes by solving appropriate differential equations, followed by determination of the burning rate in each phase. In the steady-state combustion regime, the burning rates in the gas and condensed phases are equal. This can be used to obtain the value of the burning surface temperature, an important characteristic of the combustion process.

2) The combustion mechanism for laminated or heterogeneous systems is governed not only by mass transfer in the gas phase via diffusion of components, but also by heat exchange between the components in the condensed phase. These factors together with appropriate kinetics determine the combustion regimes of energetic materials.

3) The adequacy of the mathematical model for the combustion phenomenon under study could not be proved by a comparison of the values of arbitrarily chosen combustion characteristics or parameter dependencies. For this purpose, a number of calculated characteristics showing qualitative and quantitative agreement with the experiment should be used. In particular, these characteristics can be dependencies of the burning rate and its sensitivity on pressure, initial temperature, concentration, and physicochemical properties of the components. Comparison of theoretical results with different kinds of experimental data reliably determines the applicability range of the mathematical model for further use in predicting propellant combustion characteristics.

References

[1]Zeldovich, Ya. B., Barenblatt, G. I., Librovich, V. B., and Makhviladze, G. M., *Mathematical Theory of Combustion and Explosion*, Nauka, Moscow, 1980.

[2]Williams, F. A., *Combustion Theory*, Addison-Wesley, Reading, MA, 1965.

[3]Kuo, K. K., and Summerfield, M. (eds.), *Fundamentals of Solid-Propellant Combustion*, Vol. 90, Progress in Astronautics and Aeronautics, AIAA, New York, 1984.

[4]Novozhilov, B. V., "The Velocity of Exothermic Reaction Front Propagation in the Condensed Phase," *Doklady Akademii Nauk SSSR*, Vol. 141, No. 1, 1961, pp. 151–153.

[5]Andreev, K. K., *Thermal Decomposition and Combustion of Explosives*, Nauka, Moscow, 1966.

[6]Strunin, V. A., "Condensed Phase Combustion of Explosives," *Zhurnal Fizicheskoi Khimii*, Vol. 39, No. 2, 1965, pp. 433–435.

[7]Strunin, V. A., Manelis, G. B., Ponomarev, A. N., and Talroze, V. L., "The Effect of Ionizing Radiation on Combustion of AP and AP-Based Materials," *Fizikaz Gorenia i Vzryva*, Vol. 4, No. 4, 1968, pp. 584–590.

[8]Maksimov, E. I., and Merzhanov, A. G., "A Combustion Model for Nonvolatile Substances," *Doklady Akademii Nauk SSSR*, Vol. 157, No. 2, 1964, pp. 412–415.

[9]Manelis, G. B., Nechiporenko, G. N., Raevskii, A. V., Rubtsov, Yu. I., and Strunin, V. A., "Thermal Decomposition and Deflagration of Solid Boranehydrazine," *Combustion of Boron-Based Solid Propellants and Solid Fuels*, edited by K. K. Kuo, CRC Press, Boca Raton, FL, 1993, p. 348.

[10]Manelis, G. B., and Strunin, V. A., "The Mechanism of Ammonium Perchlorate Burning," *Combustion and Flame*, Vol. 17, No. 1, 1971, pp. 69–77.

[11]Strunin, V. A., and Manelis, G. B., "Temperature Sensitivity of Burning Rate of Condensed Substances," *Fizika Gorenia i Vzryva*, Vol. 11, No. 5, 1975, pp. 797–799.

[12]Novozhilov, B. V., "The Stability Criterion for Steady-State Combustion of Powder," *Zhurnal Prikladnoi Mekhaniki i Tekhnicheskoi Fiziki*, No. 4, 1965, pp. 157–160.

[13]Strunin, V. A., and Manelis, G. B., "Stability of Stationary Combustion of Explosives with the Condensed-Phase Rate-Determining Reaction," *Fizika Gorenia i Vzryva*, Vol. 7, No. 4, 1971, pp. 498–501.

[14]Manelis, G. B., and Strunin, V. A., "Mechanism and Elementary Theory of Burning of the Composite Solid Propellants," *Proceedings of the 11th International Symposium on Space Technology and Science* (Tokyo), 1975, pp. 97–104.

[15]Bokii, V. A., Strunin, V. A., Manelis, G. B., Grigorovich, Z. I., and Rosolovskii, V. Ya., "Combustion Mechanism for Hydroxylamine Perchlorate," *Fizika Forenia i Vzryva*, Vol. 15, No. 4, 1979, pp. 55–59.

[16]Manelis, G. B., Strunin, V. A., and Rubtsov, Yu. I., "Thermal Decomposition and Combustion Mechanism of Ammonium and Hydrazonium Salts," *Archivum Termodinamiki i Spalania*, Vol. 6, No. 1, 1975, pp. 51–57.

[17]Glazkova, A. P., *Catalysis of Combustion of Explosives*, Nauka, Moscow, 1976.

[18]Zhevlakov, A. F., Strunin, V. A., and Manelis, G. B., "Combustion Mechanism of Hydrazonium Nitrate and Effects of Alkali Salts Additives," *Fizika Gorenia i Vzryva*, Vol. 12, No. 2, 1976, pp. 185–191.

[19]Vilyunov, V. N., "Mathematical Theory of Steady-State Burning Rate of Condensed Substances," *Doklady Akademii Nauk SSSR*, Vol. 136, No. 1, 1961, pp. 136–139.

[20]Strunin, V. A., Firsov, A. N., Shkadinskii, K. G., and Manelis, G. B., "Combustion Regimes of Volatile Materials Decomposing in the Condensed and Gas Phases," *Fizika Gorenia i Vzryva*, Vol. 22, No. 1, 1986, pp. 40–47.

[21]Strunin, V. A., Firsov, A. N., Shkadinskii, K. G., and Manelis, G. B., "Steady-State Combustion of Decomposing and Vaporizing Condensed Substances," *Fizika Gorenia i Vzryva*, Vol. 13, No. 11, 1977, pp. 3–9.

[22]Manelis, G. B., Strunin, V. A., and Dyakov, A. P., "The Role of Heterogeneous Reactions in Combustion Mechanism of Solid Fuels," Joint Meeting of the Soviet and Italian Sections of the Combustion Inst., No. 7.4, Pisa, Italy, 1990.

[23]Bakhman, N. N., and Belyaev, A. F., *Combustion of Heterogeneous Condensed Systems*, Nauka, Moscow, 1967.

[24]Andersen, W. H., Bills, K. W., Mishuk, E., Moe, G., and Shultz, R. D., "A Model Describing Combustion of Solid Composite Propellants Containing Ammonium Nitrate," *Combustion and Flame*, Vol. 3, 1959, pp. 301–318.

[25]Rybanin, S. S., and Strunin, V. A., "Theoretical Study of Heat and Mass Exchange Between Reacting Components Separated by Gas," *Proceedings of the 5th All-Union Conference on Heat and Mass Exchange*, Vol. 2, Minsk, Russia, 1976, pp. 30–39.

[26]Dyakov, A. P., Strunin, V. A., and Manelis, G. B., "Experimental Study of the Combustion of a Laminated System with Components Separated by a Gas Layer," *Proceedings of the 4th All-Union Symposium on Combustion and Flame*, Moscow, 1977, pp. 244–248.

[27]Strunin, V. A., Firsov, A. N., Shkadinskii, K. G., and Manelis, G. B., "Heterogeneous Combustion of a Laminated System," *Fizika Gorenia i Vzryva*, Vol. 25, No. 5, 1989, pp. 25–32.

[28]Strunin, V. A., Firsov, A. N., Shkadinskii, K. G., and Manelis, G. B., "The Structure of Heterogeneous Combustion Wave in Laminated Systems," *Fizika Gorenia i Vzryva*, Vol. 26, No. 5, 1990, pp. 36–42.

[29]Strunin, V. A., Firsov, A. N., Shkadinskii, K. G., and Manelis, G. B., "The Rate and Structure of Heterogeneous Combustion Front in the Layer System," *Flame Structure*, Vol. 1, Nauka, Novosibirsk, Russia, 1991, pp. 258–261.

[30]Price, E. W., Sambamurthi, J. K., Sigman, R. K., and Panyam, R. R., "Combustion of Ammonium Perchlorate—Polymer Sandwiches," *Combustion and Flame*, Vol. 63, No. 3, 1986, pp. 381–413.

[31]Petukhova, L. B., Peregudova, T. V., Strunin, V. A., and Manelis, G. B., "Methods for Calculation of Burning Rate Dependence on Pressure," *Fizika Gorenia i Vzryva*, Vol. 25, No. 3, 1989, pp. 36–39.

[32]Strunin, V. A., Petukhova, L. B., and Manelis, G. B., "On Pressure Exponent Variations in the Combustion of Composite Propellants," *Fizika Gorenia i Vzryva*, Vol. 29, No. 2, 1993, pp. 68–72.

[33]Strunin, V. A., and Manelis, G. B., "On Variations of Combustion Characteristics for Propellants with Competitive Reactions," *Fizika Gorenia i Vzryva*, Vol. 19, No. 2, 1983, pp. 89–94.

[34]Strunin, V. A., and Manelis, G. B., "Combustion Mechanism for Composite Solid Propellants," *Fizika Gorenia i Vzryva*, Vol. 15, No. 5, 1979, pp. 24–33.

[35]Cohen, N. S., "Review of Composite Propellant Burn Rate Modeling," AIAA Paper 79-160, 1979.